Int. J. Electrochem. Sci., 7 **(2012)** 6599 - 6610

International Journal of
ELECTROCHEMICAL
SCIENCE
www.electrochemsci.org

Inhibitory Action of Non Toxic Compounds on the Corrosion Behaviour of 316 Austenitic Stainless Steel in Hydrochloric Acid Solution: Comparison of Chitosan and Cyclodextrin

A. Eddib[1], *Y. Ait Albrimi*[1], *A. Ait Addi*[1], *J. Douch, R.M. Souto*[2] *M. Hamdani*[1,*]

[1] Laboratoire de Chimie Physique, Faculté des Sciences, Université Ibn Zohr, B.P. 8106, Cité Dakhla, Agadir, Maroc.
[2] Department of Physical Chemistry, University of La Laguna, E-38205 La Laguna (Tenerife, Canary Islands), Spain.
[*]E-mail: hamdani.mohamed@gmail.com

Received: 27 April 2012 / *Accepted:* 15 May 2012 / *Published:* 1 August 2012

The inhibitory action of two non toxic organic compounds, chitosan and hydroxypropyl-beta-cyclodextrin (HP-β-CD), against the corrosion of 316 austenitic stainless steel in acidic chloride solutions was studied. Weight loss and electrochemical tests show that the inhibitory action increases with concentration of the organics, though the effect is greater with chitosan than with HP-β-CD for a given concentration. These compounds act as anodic inhibitors (by forming an adsorbing film on the metal surface and blocking the active corrosion sites), whereas the cathodic half-reaction is not significantly affected. The highest inhibition efficiency attained in 0.1 M HCl solution was 76% by using chitosan.

Keywords: Stainless steel; Acid solutions; EIS; Polarization; Corrosion inhibition

1. INTRODUCTION

Grade 316 is a type of austenitic stainless steel (SS) with low carbon content that is widely used in industrial applications due to its strength and high corrosion resistance. This steel is an iron alloy with superior corrosion resistance, though it is susceptible to localized corrosion, pitting corrosion particularly, when it is exposed to chloride-containing aqueous solutions. Hydrochloric acid and sea water are particularly aggressive environments and promote pitting corrosion. In order to prevent the corrosive attack and dissolution of the metal, most efforts involve the use of corrosion inhibitors [1-3],

though changes in the composition of the alloy [4], and the development of new processing technologies [5-7], may also lead to the fabrication of more resistant materials.

Organic compounds containing heteroatoms such as nitrogen, sulphur and oxygen atoms are potential corrosion inhibitors [8], and among them, compounds containing sulphur and nitrogen are usually more effective inhibitors in acidic media [9]. Many inhibitors are adsorbed on the surface of the metal to protect, and their adsorption is affected by the composition of the steel, the composition of the aggressive environment, and the chemical structure of the inhibitor [10,11]. The extent of this effect depends on physicochemical properties of the molecule, namely the nature of the functional groups, molecule size and geometry, and its electron density [11]. A source of increasing concern in relation to the application of corrosion inhibitors for metal protection is that most available compounds are toxic and harmful to the environment, causing pollution, and they are even hazardous to the human health. The application of green chemistry principles to the area of corrosion inhibitors is currently explored with the objective to discover eco-friendly formulations which are either non toxic or may present a very low environmental impact. Thus, such inhibitors should be biodegradable and not bio-accumulative to avoid a negative impact on the environment. In this way, several new molecules, either extracted from plants [12,13] or synthesized in the laboratory [14,15], are currently explored as alternative inhibitors for the corrosion protection of metallic materials.

In a previous work [16], the corrosion behaviour of AISI 316 stainless steel exposed to either hydrochloric or sulphuric acid solutions was investigated using potentiodynamic and chronoamperometric techniques with special focus on the characterization of the pitting susceptibility of the steel in these environments. The influence on the corrosion resistance of the material of several factors such as the nature of the acidic media and its concentration, potential cycling of the metal, potential scan rate, and the addition of chloride ions, was explored. In this contribution, the applicability of two naturally-occurring non toxic organic molecules to inhibit the corrosion of stainless steel was considered. The compounds under investigation were chitosan and hydroxypropyl-beta-cyclodextrin (HP-β-CD), and their inhibition efficiency of 316 stainless steel corrosion in HCl was determined for various concentrations of the inhibitors in the environment.

2. EXPERIMENTAL PART

2.1. Materials

An austenitic stainless steel AISI 316 (Goodfellow, Cambridge, UK) has been considered. The corrosion behaviour of the stainless steel was investigated in hydrochloric acid solutions using weight loss and electrochemical tests, namely potentiodynamic polarization and electrochemical impedance spectroscopy (EIS) measurements. The test solution for the electrochemical tests was 0.1 M HCl, both in the absence and in the presence of different concentrations of the corrosion inhibitors. Weight loss measurements were also conducted in 0.1, 0.5 and 1 M HCl solutions with and without HP-β-CD. These solutions were prepared using a laboratory grade HCl solutions. The temperature was fixed at 293 ± 1 K.

The two corrosion inhibitors, chitosan and hydroxypropyl-beta-cyclodextrin (HP-β-CD), were supplied by Roquette Frères (Lestrem, France), and they were used without further purification. The molar weight (MW) and the degree of deacetylation of chitosan were 40 KDa and 85% respectively, whereas the MW of HP-β-CD was 1500 g mol^{-1}. The chemical structures of these compounds are shown in Figure 1.

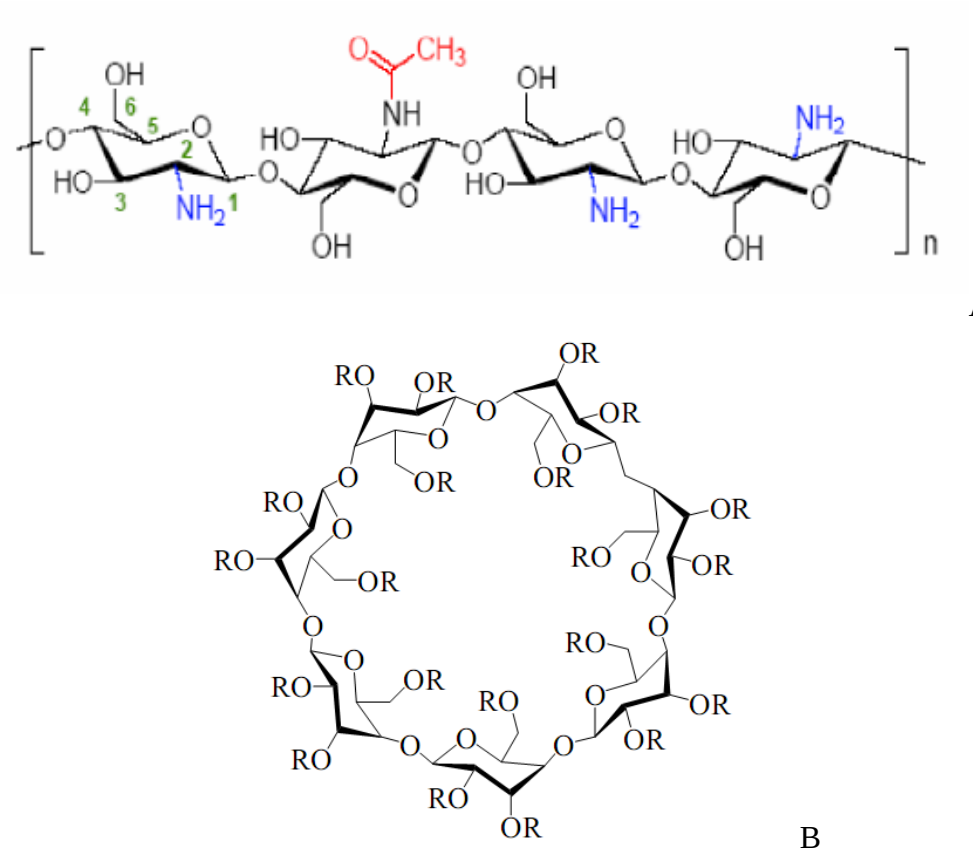

Figure 1. Molecular structures of: a) Chitosan, and b) Hydroxypropyl-beta-cyclodextrin (HP-β-CD), $(C_{42}H_{70-n}O_{35})$ $(C_3H_7O)_n$, R = H, n = 6.31.

2.2. Experimental procedures

Plates of steel with dimensions of size 1 cm x 1 cm x 0.1 cm were used for the weight loss determinations (2 cm^2 exposed). The specimens were weighed prior to immersion in 100 ml of different concentration of acid solutions at 293 K. These plates were totally immersed in the test electrolyte for 15 days, using a glass hook to hold them vertically. Samples were retrieved from the test solution every 24 hours, carefully washed with high purity water in an ultrasound bath and subsequently dried in the oven, prior to weight loss measurements. The plates were reweighed up to $1*10^{-4}$ g for determining corrosion rate. The difference in weight of the SS plates was then taken as the weight loss. The weight loss tests were reproduced twice to guarantee the reproducibility of the results. The accuracy of the method was within 5%. All the tests were conducted in the naturally-aerated

solutions at 293 K using a thermostat-cooling condenser for the temperature control. The inhibition efficiency, *E*(%), was determined by using the following equation:

$$E(\%) = \frac{W_0 - W_i}{W_0} \times 100 \quad (1)$$

where W_i and W_0 are the weight loss value in presence and absence of inhibitor, respectively [17].

Electrochemical measurements were carried out in a conventional three-electrode single compartment glass cell using a potentiostatic electrochemical set (Voltalab PRZ 100 Radiometer-Analytical) operating under computer control. The potential of the working electrode was measured against a saturated calomel electrode (SCE) (0.240 V vs. SHE). The SCE was connected to the cell through a KCl agar-agar salt bridge, the tip of which was placed as close as possible to the surface of the working electrode in order to minimize the solution resistance between the test and reference electrodes. Plates of steel with dimensions of size 1 cm × 2 cm × 0.1 cm, have been used as the working electrodes in 50 ml of the aerated test solution containing HCl, both in the absence and in the presence of the corrosion inhibitors. A single electrode face was in contact with the electrolyte (2 cm^2). The opposite face was covered with an inactive and non conductive varnish. A more detailed description of electrochemical experiments can be found elsewhere [16]. The inhibition efficiency was evaluated from the measured I_{corr} values using [18]:

$$E(\%) = \frac{I_0 - I}{I_0} \times 100 \quad (2)$$

where I_0 and I are the corrosion current densities determined by the intersection of the extrapolated Tafel lines at the corrosion potential for the steel in uninhibited and inhibited acid solution, respectively. All measurements were performed at 293 K.

EIS measurements were performed in 0.1 M hydrochloric acid solutions which contained different concentrations of corrosion inhibitors. An *ac* voltage signal with amplitude of 5 mV around the open-circuit potential of the metal in the solution was applied in frequency range of 100 kHz to 10 mHz. Impedance spectra are represented in the form of both Nyquist (imaginary component of the impedance as a function of the real component) and Bode (logarithm of the impedance modulus |*Z*| and phase angle ϕ as a function of the logarithm of the frequency *f*) plots. A new specimen was used for each run. The experimental procedures and conditions employed in the EIS study were similar to those described previously [19,20]. The values of *E*(%) were calculated using the following equation [17]:

$$E(\%) = \frac{R_p - R_{p0}}{R_{p0}} \times 100 \quad (3)$$

where R_{p0} and R_p are the polarization resistance values determined for the steel in uninhibited and inhibited acid solution, respectively.

3. RESULTS AND DISCUSSION

3.1. Weight loss determinations

The gravimetric losses were determined for 316 stainless steel in 0.1, 0.5 and 1 M HCl, with and without of 1 mM HP-β-CD, over a period of 15 days. Chitosan was tested as corrosion inhibitor in 0.1 M HCl exclusively, due to poor solubility of this molecule in more acidic media. Thus, the comparison of the two corrosion inhibitors under consideration was only possible in 0.1 M HCl base solution

The amount of material loss depended on the concentration of the acid and the nature and the concentration of the inhibitor. The greatest weight loss was found in the case of the inhibitor-free 1 M HCl solution ($1.10*10^{-3}$ g cm^{-2} day^{-1}, at 293 K). The mean corrosion rates obtained for 15 days immersion period in inhibitor-free and in $1*10^{-3}$ M inhibitor-containing solutions are summarized in Table 1. This parameter could be approximated by a linear equation of the form: $y = a \times t$, where y represents the mass loss in expressed in g cm^{-2}, t is the immersion time in days, and a is the mean corrosion rate in g cm^{-2} day^{-1}. The fit regression parameters (R^2) were close to unity. It can be observed that the weight loss varied linearly with immersion period in all the test conditions, an indication that the steel sample did not present insoluble products on its surface. The same observation was made by Singh and Qurashi for the inhibition of the corrosion of mild steel in hydrochloric acid and sulphuric acid solutions by an extract taken from *murraya koenigii* leaves [21]. It was also noticed that after 2 days immersion of the steel in 1 M HCl, a greenish color appeared in the solution, characteristic of Cr^{3+} species, which became more intense as time further elapsed. This result indicated the release of metallic ions in the solution.

Table 1. Corrosion rates (g cm^{-2} day^{-1}) and inhibition efficiencies E(%) for 316 stainless steel in different concentrations of HCl with and without the addition of inhibitors. They were determined from weight loss measurements over 15 days. Inhibition efficiencies are given between brackets.

	[HCl], M		
	0.1	0.5	1.0
Blank solution	$0.25*10^{-3}$	$0.46*10^{-3}$	$1.10*10^{-3}$
1 mM HP-β-CD	$0.08*10^{-3}$ (68)	$0.22*10^{-3}$ (52)	$0.86*10^{-3}$ (22)
1 mM chitosan	$0.02*10^{-3}$ (92)	-*	-*

***** Chitosan is not soluble in strong acidic media

On the other hand, it can be observed that the inhibition efficiency of 1 mM HP-β-CD decreases from 68 to 22% when the HCl concentration was increased from 0.1 to 1 M. And for equal inhibitor concentrations (1 mM) in the test solution, chitosan exhibited the highest inhibition efficiency (92%) compared to HP-β-CD (68%).

3.2. Polarization measurements

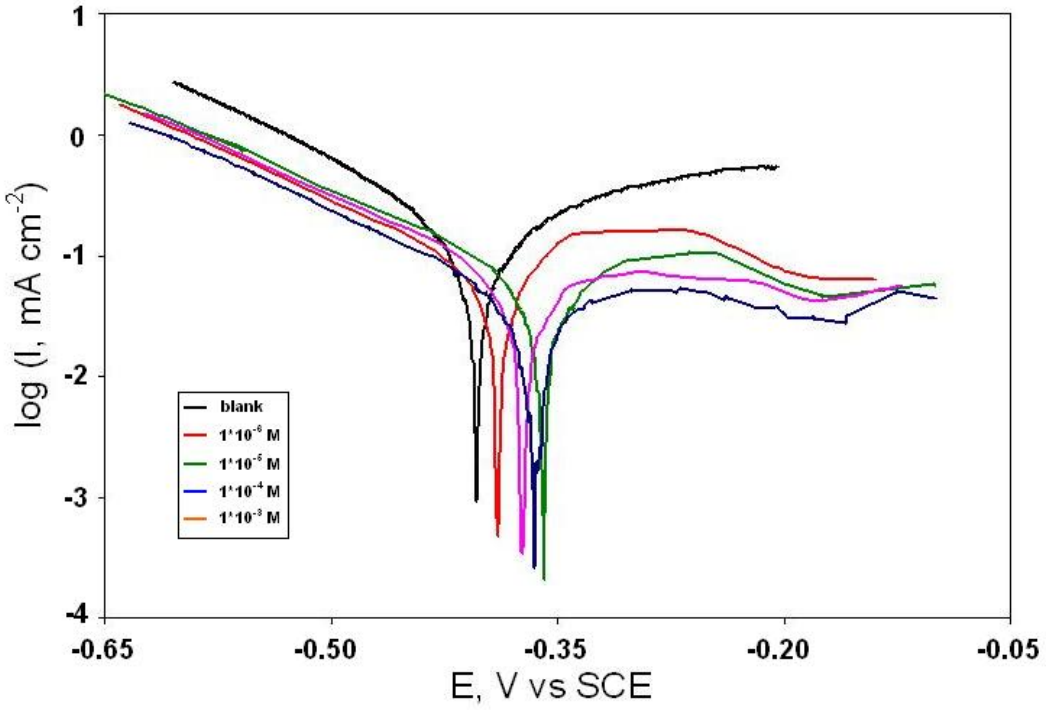

Figure 2. Potentiodynamic polarization curves of 316 stainless steel in 0.1 M HCl without and with various concentrations of chitosan as indicated in the figure. v =1 mV s^{-1}.

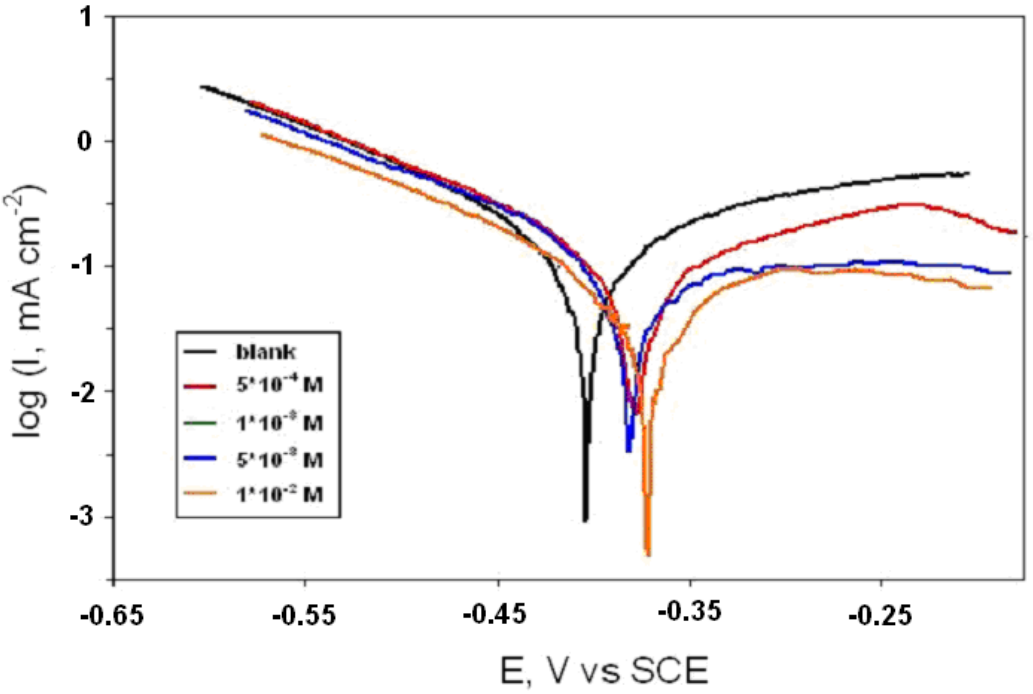

Figure 3. Potentiodynamic polarization curves of 316 stainless steel in 0.1 M HCl without and with various concentrations of HP-β-CD as indicated in the figure. v =1 mV s^{-1}.

The electrolyte used to test the electrochemical behaviour of AISI 316 austenitic stainless steel electrodes was 0.1 M HCl. The metal samples were immersed in the test solution until a steady-state open circuit potential (E_{OCP}) was reached every time (after *ca.* 30 min). Figures 2 and 3 show the potentiodynamic curves obtained in both inhibitor-free and inhibitor-containing solutions of various concentrations. The cathodic branch was always first recorded by shifting the electrode potential from E_{OCP} to more negative values at the sweep rate of 1 mV s^{-1}. Next, the anodic branch was recorded from E_{OCP} to the corresponding positive potential limit at the same scan rate.

Table 2. Electrochemical parameters and the corresponding inhibition efficiencies of AISI 316 austenitic stainless steel specimens in 0.1 M HCl as a function of chitosan concentration.

$c_{chitosan}$, mM	E_{corr}, mV SCE	I_{corr}, µA cm^{-2}	$-\beta_c$, mV $decade^{-1}$	E(%)
0	−426	129	128	–
0.001	−391	62	171	52
0.01	−359	59	184	54
0.1	−373	57	175	56
11	−365	38	173	71

Table 3. Electrochemical parameters and the corresponding inhibition efficiencies of AISI 316 austenitic stainless steel specimens in 0.1 M HCl as a function of HP -β- CD concentration.

$c_{HP\text{-}\beta\text{-}CD}$, mM	E_{corr}, mV SCE	I_{corr}, µA cm^{-2}	$-\beta_c$, mV $decade^{-1}$	E(%)
0	−426	76	166	–
0.1	−391	58	130	24
0.5	−394	49	116	36
1	−381	42	153	45
5	−377	38	181	50
10	−373	35	133	54

The kinetic parameters were thus determined from the potentiodynamic measurements, including the corrosion potential, E_{corr}, the corrosion current, I_{corr}, the cathodic Tafel slope, β_c, and the inhibition efficiency, E(%), which are listed in Tables 2 and 3 for each inhibitor. It can be observed that the cathodic branches of the current-potential curves were almost parallel in all cases. This finding supports that hydrogen evolution is activation-controlled. That is, the mechanism of the hydrogen reduction is not affected by the presence of the organic molecules in the electrolyte. Further inspection of the polarization curves reveals that the corrosion potential was shifted towards more anodic potentials with the increase in the concentration of the inhibitor. Furthermore, the anodic current densities decreased when the corrosion inhibitor concentrations increased, and the magnitude of such was bigger with higher inhibitor concentrations. This behaviour reflects the inhibitive action of the testing corrosion inhibitors. The results indicate that the two compounds act predominantly as anodic inhibitors through the physical blockage of the available surface area [22]. Current oscillations could

also be observed in the passivity region, that is, between E_{corr} and E_{pit} (cf. Figures 2 and 3). Similar observations have already been reported in the case of austenitic steels with high manganese contents [23].

3.3. Electrochemical impedance spectroscopy

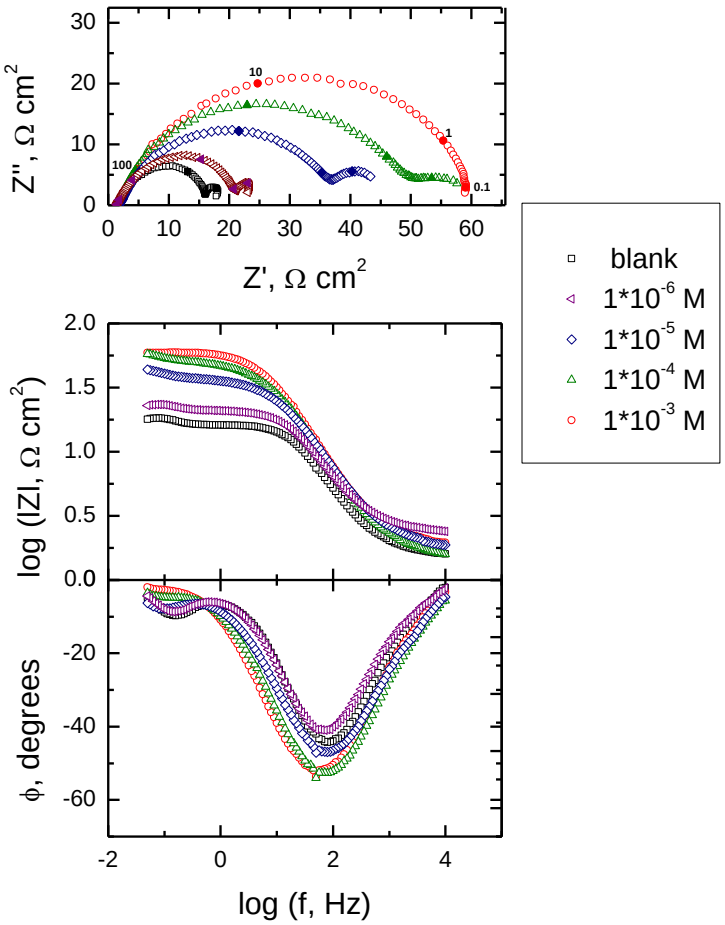

Figure 4. Impedance spectra of 316 stainless steel samples in 0.1 M HCl without and with various concentrations of chitosan at 293 K. (Frequencies are indicated in Nyquist plot)

Measurements of electrochemical impedance have been carried out at open circuit potential (E_{corr}) after immersion of the 316 SS samples in 0.1 M HCl solution without and with various concentrations of the inhibiting molecules, at room temperature. The Nyquist and Bode impedance plots obtained are shown in Figures 4 and 5. The uncompensated solution resistance R_s is 2.0 ± 0.5 Ω cm^2 in these systems. The Nyquist graphs show depressed semicircles; that is, constant phase elements, CPE, accounting for the heterogeneity of the metal surface, had to be employed to describe the double layer characteristics of the systems. It is observed that the Nyquist plots exhibit a second capacitive loop in the low frequency range (LF) for the steel electrode in 0.1 M HCl, a result that has also been found by other groups when the chromium content in the steel exceeds 17 wt% in the presence of 1 wt% Mo [4,24-27]. On the other hand, the addition of the organic compounds affects the

electrochemical properties of the system, as evidenced by changes in the shape of the EIS spectra in the low frequency limit.

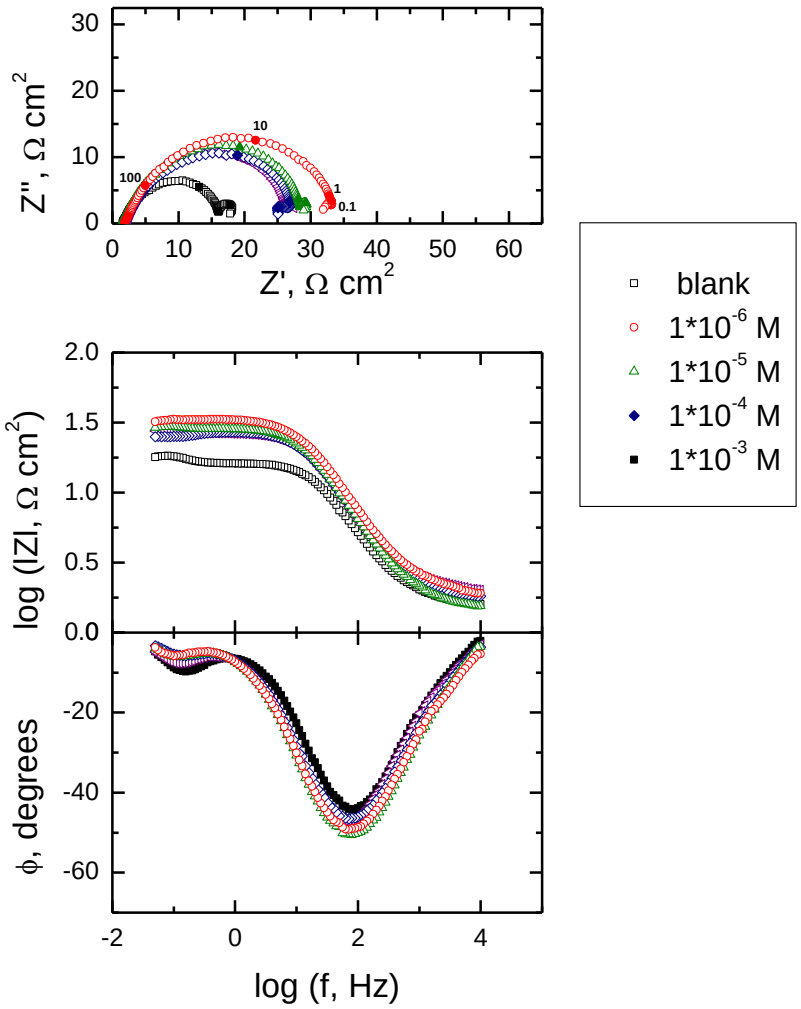

Figure 5. Impedance spectra of 316 stainless steel samples in 0.1 M HCl without and with various concentrations of HP-β-CD at 293 K. (Frequencies are indicated in Nyquist plot)

These changes are dependent on the concentration of the inhibitor, and can be observed as the progressive disappearance of the second time constant occurring in the low frequency limit. That is, only one time constant was observed in the spectra for the higher inhibitor concentrations considered, whereas two time constants were found in the blank solution and in those solutions of the inhibitors at a smaller concentration. In this way, the blocking effect of the inhibitors is evidenced in the sequence of spectra displayed in Figures 4 and 5. Surface layers with protective properties are formed from the interaction of either chitosan or hydroxypropyl-beta-cyclodextrin when present in the 0.1 M HCl solution.

Table 4. Impedance data for AISI 316 austenitic stainless steel specimens in 0.1 M HCl as a function of chitosan concentration.

$c_{chitosan}$, M	R_p, Ω cm^2	f, Hz	C_{dl}, µF cm^{-2}	E(%)
0	15.3	22	474	-
1*10^{-6}	21.8	17.2	425	30
1*10^{-5}	39.5	10.0	403	61
1*10^{-4}	53.3	8.3	360	71
1*10^{-3}	63.4	7.1	354	76

Table 5. Impedance data for AISI 316 austenitic stainless steel specimens in 0.1 M HCl as a function of HP-β-CD concentration.

$c_{HP\text{-}\beta\text{-}CD}$, M	R_p, Ω cm^2	f, Hz	C_{dl}, µF cm^{-2}	E(%)
0	15.3	22	474	-
1*10^{-6}	25.2	13.7	460	39
1*10^{-5}	27.4	13.4	433	44
1*10^{-4}	28.0	13.8	412	45
1*10^{-3}	33.5	11.7	406	54

The corrosion resistance of the samples was established from the polarization resistance, R_p, values determined from the impedance spectra. R_p can be directly estimated from the diameter of the first semicircle disclosed at high and intermediate frequencies (HF and IF) obtained from the experimental Nyquist plots after extrapolation of the data towards the real axis at low frequencies [18]. The values of R_p are found to increase with increasing concentrations of the inhibitor compounds as shown in Tables 4 and 5._ In case of the chitosan inhibitor, the diameter of the loop appearing in the low frequency range in Nyquist plots increased with the increasing the inhibitor concentration, except for the highest value of the concentration tested when the arc disappeared. For the other inhibitor, the second loop is present but its diameter is not depending on the inhibitor concentration. Pardo et al [4] have attributed the first capacitive loop to the combined effect of the double layer capacitance and iron dissolution from the metal since Fe is the major alloying element. The second loop was attributed to oxidation and subsequent adsorption of Mo species. They also showed that the later arc disappeared when the Mo content was less than 2 wt% (i.e., in AISI 304 stainless steel) and it was replaced by an inductive arc at the lowest frequencies.

The double layer capacitance, $C_{dl,}$ values were calculated from the frequency at apex on Nyquist plot, i.e. when imaginary component of impedance was maximum ($-Z_{im,\,apex}$)

$$C_{dl} = \frac{1}{2\pi\ f_{apex}\ R_p} \qquad (4)$$

The values of the double layer capacitance, C_{dl}, the frequencies at the apex in the Nyquist plots, and the inhibitor efficiency values for each solution determined using equation (3) are given in Tables

4 and 5. It is observed that the absolute impedance at low frequencies in Bode plot R_p values increased while C_{dl} values decrease with the concentration of the inhibitors. The increase of R_p confirms the higher protection with increasing the concentration of inhibitors**,** which is related to its adsorption on the SS surface. On the other hand, the decrease of values can be attributed to the gradual replacement of water molecules by the adsorption of the organic compounds on the electrode surface, which hinders metal dissolution [28]. These observations suggest the inhibitor molecules function by adsorption on the metal surface thereby causing R_p values to increase and C_{dl} values to decrease accordingly.

Electrochemical results support that chitosan is a more efficient inhibitor than HP-β-CD, an observation that agrees well with the results from the weight loss technique. The essential effect of the corrosion inhibitors is due to the electron donor groups (O and N for chitosan, and O for the HP-β-CD) in the tested environments. The presence of free electrons and double bonds in the molecules favoured their interaction with a positively charged surface [29].

4. CONCLUSIONS

Chitosan and hydroxypropyl-beta-cyclodextrin inhibited the corrosion of 316 austenitic stainless steel in acidic hydrochloric acid solutions at 293 K. These inhibitors act through an anodic mode of inhibition as evidenced by potentiodynamic polarization studies. The corrosion inhibition is due to the presence of heteroatoms in the inhibitor formulations which provide interacting electrons with the steel surface.

Electrochemical impedance data are consistent with a reduction in the charge transfer reaction rate for the anodic process as result of the interaction of the organic compound with the metallic surface, which is evidenced by increasing polarization resistance and decreasing double layer capacitance values. These organic compounds are adsorptive inhibitors and they physically block the surface of stainless steel from the attack of the aggressive species in the electrolytic environment.

ACKNOWLEDGEMENTS

The authors gratefully acknowledge the support of this work by the Pôle de Compétences Electrochimie-Corrosion et Chimie Analytique (PECCA), Ministère de l'Education Nationale, de l'Enseignement Supérieur, de la Formation des Cadres et de la Recherche Scientifique (Maroc). The Ministerio de Ciencia e Innovación (Madrid, Spain) and the European Regional Development Fund (Brussels, Belgium) assisted the publication of this work within the framework of Project CTQ2009-12459.

References

1. B. Sanyal, *Prog. Org. Coat.* 9 (1981) 165-236.
2. H. Deng, H. Nanjo, P. Qian, Z. Xia, I. Ishikawa, T.M. Suzuki, *Electrochim. Acta* 53 (2008) 2972-2983.
3. M.A. Amin, K.F. Khaled, Q. Mohsen, H.A. Arida, *Corros. Sci.* 52 (2010) 1684-1695.

4. A. Pardo, M.C. Merino, A.E. Coy, F. Viejo, R. Arrabal, E. Matykina, *Corros. Sci.* 50 (2008) 780-794.
5. G.T. Burstein, I.M. Hutchings, K. Sasaki, *Nature* 407 (2000) 885-887.
6. G.T. Burstein, K. Sasaki, I.M. Hutchings, *Electrochem. Solid State Commun***.** 6 (2003) D13-D15.
7. G.T. Burstein, R.M. Souto, *J. Electrochem. Soc.* 151 (2004) B537-B542.
8. L Herrag, A. Chetouani, S. Elkaderi, B. Hammouti, A. Aouniti, *Portugaliae Electrochim. Acta* 26 (2008) 211-220.
9. S. Muralidharan, K.L.N. Phani, S. Pitchumani, S. Ravichandran, S.V.K. Iyer, *J. Electrochem. Soc.* 142 (1995) 1478-1483.
10. B.M. Braveen, T.V. Vankatesh, *Int. J. Electrochem. Sci.* 4 (2009) 267-275.
11. S.S. Abdel Rehim, M.A.M. Ibrahim, K.F. Khalid, *J. Appl. Electrochem.* 29 (1999) 593-599.
12. A. Bouyanzer, B. Hammouti, L. Majidi, *Mater. Letters* 60 (2006) 2840-2843.
13. F.S. de Souza, A. Spinelli, *Corros. Sci.* 51 (2009) 642-649.
14. M.Outirite, M. Lagrenée, M. Lebrini, M. Traisnel, C. Jama, H. Vezin, F. Bentiss, *Electrochim. Acta* 55 (2010) 1670-1681.
15. M. Mahdavian, S. Ashhari, *Electrochim. Acta* 55 (2010) 1720-1724.
16. Y. Ait Albrimi, A. Eddib, J. Douch, Y. Berghoute, M. Hamdani, R.M. Souto, *Int. J. Electrochem. Sci.* 6 (2011) 4614-4627.
17. M.A. Quraishi, A. Singh, V.K. Singh, D.K. Yadav, A.K. Singh, *Mater. Chem. Phys.*122 (2010) 114-122.
18. D.-Q. Zhang, Z.-X. An, Q.-Y. Pan, L.-X. Gao, G.-D. Zhou, *Appl. Surf. Sci.* 253 (2006) 1343-1348.
19. E. Laouini, M. Hamdani, M.I.S. Pereira, J. Douch, M.H. Mendonça, Y. Berghoute, R.N. Singh, *Int. J. Hydrogen Energy* 33 (2008) 4936-4944.
20. E. Laouini, M. Hamdani, M.I.S. Pereira, J. Douch, M.H. Mendonça, Y. Berghoute, R.N. Singh, *J. Appl. Electrochem.* 38 (2008) 1485-1494.
21. A.K. Singh, M.A. Quraishi, *Corros. Sci.* 51 (2009) 2752-2760.
22. S.S. Abd El Rehim, H.H. Hassan, M.A. Amin, *Corros. Sci.* 46 (2004) 1071-1082.
23. A. Pardo, M.C. Merino, A.E. Coy, F. Viejo, R. Arrabal, E, Matykina, *Corros. Sci*. 50 (2008) 1796-1806.
24. K. Sugimoto, Y. Sawada, *Corros. Sci.* 17 (1977) 425-445.
25. M. Keddam, O. R. Mattos, H. Takenouti, *Electrochim. Acta* 31 (1986) 1159-1165.
26. I. Annergren, M. Keddam, H. Takenouti, D. Thierry, *Electrochim. Acta* 38 (1993) 763-771.
27. I. Annergren, M. Keddam, H. Takenouti, D. Thierry, *Electrochim. Acta* 42 (1997) 1595-1611.
28. F. Bentiss, M. Lebrini, M. Lagrenée, *Corros. Sci.* 47 (2005) 2915-2931.
29. M. Bouklah, B. Hammouti, A. Aouniti, T. Benhadda, *Prog. Org. Coat.* 49 (2004) 225-228.